Mechanisms of Photo-oxidation of NADH Model Compounds by Oxygen

Shunichi Fukuzumi,* Masashi Ishikawa, and Toshio Tanaka
Department of Applied Chemistry, Faculty of Engineering, Osaka University, Suita, Osaka 565, Japan

When an oxygen-saturated acetonitrile (MeCN) solution containing the NADH model compound, 9,10-dihydro-10-methylacridine ($AcrH_2$), is irradiated with u.v. light firstly in the presence and secondly in the absence of perchloric acid ($HClO_4$), $AcrH_2$ is oxidized by oxygen to yield the 10-methylacridinium ion ($AcrH^+$) and 10-methyl-9-acridone (Acr=O) respectively, and reduction of oxygen yields hydrogen peroxide. The u.v. irradiation of a neutral aqueous solution containing 1-benzyl-1,4-dihydronicotinamide (BNAH) also results in the oxidation of BNAH by oxygen to yield BNA^+ and H_2O_2. Kinetic studies and detection of radical intermediates by e.s.r. spectroscopy have revealed that the photo-oxidation of NADH model compounds by oxygen proceeds *via* radical-chain reactions, which are initiated by electron transfer from the singlet excited state of NADH model compounds to oxygen. The chain carrier for the photo-oxidation of $AcrH_2$ in the presence of $HClO_4$ in MeCN as well as for the photo-oxidation of BNAH in a neutral aqueous solution is hydroperoxy radical ($HO_2^{\cdot}$), while acridinylperoxy radical ($AcrO_2^{\cdot}$) acts as a chain carrier for the photo-oxidation of $AcrH_2$ in the absence of $HClO_4$ in MeCN.

Although no photo-oxidation of $AcrH_2$ by oxygen occurs under visible-light irradiation, $AcrH_2$ is efficiently oxidized to $AcrH^+$ in the presence of a flavin analogue used as a sensitizer, in MeCN under otherwise identical conditions. The flavin-sensitized photo-oxidation of $AcrH_2$ by oxygen proceeds *via* one-electron reduction of a flavin analogue by $AcrH_2$ followed by the efficient oxidation of the reduced flavin by oxygen without the appreciable contribution of radical-chain processes.

Reduced nicotinamide adenine dinucleotide (NADH) plays a vital role as the electron source in the reduction of oxygen by the respiratory chain.[1] Without appropriate catalysts such as flavin and its analogues,[2,3] NADH itself is stable to oxygen unless either oxygen or NADH is activated. An activated-oxygen species, singlet oxygen, can oxidize NADH to yield NAD^+ and H_2O_2.[4] U.v. irradiation of NADH in the presence of oxygen also results in the oxidation of NADH to yield NAD^+ and H_2O_2.[5–7] However, the mechanisms of photo-oxidation of NADH and the model compounds are not fully understood. For example, the singlet excited state of NADH is known to be oxidized by electron transfer to oxygen to produce the superoxide anion $O_2^{-\cdot}$, but the quantum yield is 10^5 and 10^6 times smaller than that for the NAD^+ formation.[6,7] The effect of acid on the photo-oxidation of NADH and the model compounds has also not been reported, since they decompose due to acid-catalysed hydration.[8]

This work reports mechanistic studies on the photo-oxidation of the NADH model compounds, $AcrH_2$ and BNAH, by oxygen under u.v. irradiation in acetonitrile (MeCN) and/or H_2O, as well as the photocatalytic oxidation of $AcrH_2$ by oxygen in the presence of a flavin analogue used as a sensitizer under visible-light irradiation in MeCN and H_2O. The effect of an acid ($HClO_4$) which causes the change in the mechanism of the photo-oxidation is also reported by using an acid-stable NADH model compound, $AcrH_2$.[9]

Experimental

Materials.—Preparation of 9,10-dihydro-10-methylacridine ($AcrH_2$) and 1-benzyl-1,4-dihydronicotinamide (BNAH) were described elsewhere.[10] 10-Methylacridinium perchlorate ($AcrH^+ClO_4^-$) was prepared by the addition of $Mg(ClO_4)_2$ to 10-methylacridinium iodide in H_2O. [9,9-$^2H_2$]-9,10-Dihydro-10-methylacridine ($AcrD_2$) was prepared by $LiAlD_4$ (sold as 98 atom % D by Aldrich) reduction of 10-methyl-9-acridone.[11] Riboflavin 2′,3′,4′,5′-tetra-acetate (RFTA) was prepared by the literature method.[12] 10-Methyl-9-acridone (Acr=O), perchloric acid (70%), electron acceptors (fumaronitrile, diethyl fumarate), and sodium iodide were obtained commercially. Potassium ferrioxalate, used as an actinometer, was prepared according to the literature[13] and was purified by recrystallization from hot water. Acetonitrile used as a solvent was purified and dried by the standard procedure.[14]

Photo-oxidation of NADH Model Compounds by Oxygen.—Typically, $AcrH_2$ (2.5×10^{-5} mol) was added to an n.m.r. tube containing CD_3CN (0.5 cm^3) in the presence of $HClO_4$ (1×10^{-3} mol) and H_2O (2.6 mol dm^{-3}). After the reactant solution had been saturated with oxygen, it was irradiated with a high-pressure mercury lamp for 25 h. The oxidized product was identified by comparing the ^1H n.m.r. spectrum of the resulting solution with that of $AcrH^+$ [δ/ppm: 4.62 (3 H, Me)]. The photo-oxidation of $AcrH_2$ by oxygen was also carried out in the absence of $HClO_4$ and H_2O in CD_3CN under conditions otherwise identical with those described above. The oxidized product was identified by comparison with the ^1H n.m.r. spectrum of 10-methyl-9-acridone (Acr=O) [δ/ppm: 3.98 (3 H, Me)]. The ^1H n.m.r. spectroscopic measurements were carried out using a Japan Electron Optics JNM-PS-100 ^1H n.m.r. spectrometer (100 MHz).

The photo-oxidation of NADH model compounds ($AcrH_2$ and BNAH) by oxygen under irradiation with light from an Ushio Model U1-501 Xenon lamp through a Toshiba UV-D33S filter were also monitored by the rise of the absorption band due to oxidized species [$AcrH^+$ (λ 400 nm, ε 4.0×10^3 mol^{-1} dm^3 cm^{-1}), Acr=O ($\lambda_{max.}$ 400 nm, $\varepsilon_{max.}$ 8.64×10^3 mol^{-1} dm^3 cm^{-1}) and BNA^+ ($\lambda_{max.}$ 270 nm, $\varepsilon_{max.}$ 3.84×10^3 mol^{-1} dm^3 cm^{-1})] or the decay of the absorption band due to BNAH ($\lambda_{max.}$ 350 nm, ε 6.00×10^3 mol^{-1} dm^3 cm^{-1}). The amount of reduction product, H_2O_2, was determined by the standard method (titration against iodide ion);[15] the solution of the product mixture was

treated with excess amounts of NaI and the amount of I_3^- formed was determined by visible spectroscopy ($\lambda_{max.}$ 365 nm, $\varepsilon_{max.}$ 2.8×10^4 mol^{-1} dm^3 cm^{-1}).[16]

The photo-oxidation of $AcrH_2$ by RFTA (9.2×10^{-5} mol dm^{-3}) in the presence of $HClO_4$ (1.0×10^{-3} mol dm^{-3}) in deoxygenated MeCN/H_2O (5:1 v/v) under light irradiation through a Toshiba Y-43 filter, which eliminated radiation below 400 nm, was monitored by the decay of the absorption band due to RFTA ($\lambda_{max.}$ 444 nm). Alternatively, the photo-oxidation of $AcrH_2$ with oxygen, catalysed by RFTA (9.2×10^{-5} mol dm^{-3}) in the presence of $HClO_4$ (1.0×10^{-3} mol dm^{-3}) in air- or oxygen-saturated MeCN–H_2O (5:1 v/v), was monitored by the rise of the absorption band due to $AcrH^+$ (λ 400 nm, ε 4.0×10^3 mol^{-1} dm^3 cm^{-1}). The amount of H_2O_2 was determined by the method described above.[16]

Quantum-yield Determinations.—A standard actinometer (potassium ferrioxalate)[13] was used for the quantum-yield determinations of the photochemical reactions of $AcrH_2$ and BNAH with oxygen. In the case of direct irradiation of $AcrH_2$ or BNAH, the quantum yield was determined under filtered light (220 nm $< \lambda <$ 440 nm) since the effect of monochromatized light was too weak to discriminate between the photochemical rate and the rate of thermal oxidation of $AcrH_2$ by oxygen, in the presence of $HClO_4$ in MeCN, or the hydration of BNAH in a neutral aqueous solution. Thus, the actinometry experiments were carried out at the same incident light intensity by using the same filter as employed in the photo-oxidation of $AcrH_2$ and BNAH. Since light absorption by the actinometer, $AcrH_2$ and BNAH is incomplete in each wavelength region, depending on the concentration, the fraction of light absorbed by the actinometer, $AcrH_2$ and BNAH must be considered explicitly.[17] The concentration of ferrous ions [Fe^{2+}] formed in the irradiated solution of the actinometer through the filter is then given by equation (1), where C is a constant used to obtain the

$$[Fe^{2+}] = C\varphi_0 t \int_0^\infty \chi(\lambda)F(\lambda)[1 - \exp(-2.3A_\lambda^0)]d\lambda \quad (1)$$

absolute light intensity absorbed by the actinometer, φ_0 is the quantum yield for the actinometer, taken as 1.18 which is the average value between 365 nm and 436 nm,[13] t is the irradiation time, $\chi(\lambda)$ is the relative emittant light intensity at wavelength λ, determined by using rhodamine 6G as a standard, $F(\lambda)$ is the wavelength dependence of the transmitting efficiency of the filter, and A_λ^0 is the absorbance of the actinometer at wavelength λ. Similarly, the quantum yields φ for the photochemical reactions of $AcrH_2$ and BNAH with oxygen are given by equations (2) and (3), respectively, where A_λ is the absorbance of

$$\varphi = [AcrH^+]/\left\{Ct \int_0^\infty \chi(\lambda)F(\lambda)[1 - \exp(-2.3A_\lambda)]d\lambda\right\} \quad (2)$$

$$\varphi = \Delta[BNAH]/\left\{Ct \int_0^\infty \chi(\lambda)F(\lambda)[1 - \exp(-2.3A_\lambda)]d\lambda\right\} \quad (3)$$

$AcrH_2$ or BNAH at wavelength λ, and Δ[BNAH] is the concentration of BNAH consumed in the photochemical reaction. The C value was determined from the actinometry experiments by substituting [Fe^{2+}], φ_0, t, and the integral term (calculated by the numerical integration) into equation (1). With the C value, the quantum yields, φ, for the photo-oxidation of BNAH and $AcrH_2$ by oxygen were determined by numerical integration using equations (2) and (3), respectively.

In the case of the RFTA-sensitized reaction, the quantum yield was determined for filtered visible light (λ > 400 nm) at wavelengths at which only RFTA is excited. In such a case, the amount of ferrous ions [Fe^{2+}] formed in the irradiated solution of the actinometer through the filter is given by equation (4),

$$[Fe^{2+}] = Ct \int_0^\infty \varphi_\lambda^0 \chi(\lambda)F(\lambda)[1 - \exp(-2.3A_\lambda^0)]d\lambda \quad (4)$$

where φ_λ^0 is the quantum yield of the formation of Fe^{2+}, which varies with λ for longer wavelengths and is placed, therefore, inside the integral term. The quantum yield, φ, for the RFTA-sensitized reaction of $AcrH_2$ is given by equation (2). However, the quantum yield for the photochemical reaction in the absence of oxygen is given by equation (5), where Δ[RFTA] is the

$$\varphi = \Delta[RFTA]/\left\{Ct \int_0^\infty \chi(\lambda)F(\lambda)[1 - \exp(-2.3A_\lambda)]d\lambda\right\} \quad (5)$$

amount of RFTA consumed by the photochemical reaction and A_λ is the absorbance of RFTA at wavelength λ. The φ values in equations (2) and (5) were determined by the numerical integration using the C value which was determined by the numerical integration in equation (4).

Fluorescence Quenching of $^1AcrH_2$*.—Quenching experiments of the $AcrH_2$ fluorescence were performed using a Hitachi 650-10S fluorescence spectrophotometer. The excitation wavelength was 285 nm for $AcrH_2$. The monitoring wavelength corresponds to the maximum of the emission band ($AcrH_2$, 385 nm). Relative emission intensities were measured for MeCN solutions of $AcrH_2$ (5.0×10^{-5} mol dm^{-3}) with a quenching agent at various concentrations. The shape did not change but intensity of the emission spectrum did on the addition of the quenching agent. The Stern–Volmer relation [equation (6)]

$$I_f^0/I_f = 1 + k_q\tau[Q] \quad (6)$$

was obtained for the ratio of the emission intensities in the absence and presence of a quencher, I_f^0/I_f, and the quenching agent concentration, [Q]. The fluorescence lifetime τ of $^1AcrH_2$* has been reported as 14 ns.[18]

Oxidation of $AcrH_2$ *by Oxygen, Initiated by the Fenton Reaction.*—Rates of the oxidation of $AcrH_2$ and $AcrD_2$ by oxygen in the presence of H_2O_2, $FeCl_2$, and $HClO_4$ in MeCN containing H_2O (2.6 mol dm^{-3}) at 298 K were followed by the rise of the absorption band due to $AcrH^+$. The kinetic measurements were carried out under pseudo-first-order conditions where the concentrations of oxygen, $HClO_4$, and H_2O_2 were maintained in excess of [$AcrH_2$]. Pseudo-first-order rate constants, k_{obs}, were determined by least-squares curve fitting, using a microcomputer.

Electron Spin Resonance Measurements.—The e.s.r. measurements were carried out by using a JEOL X-band spectrometer (JES-ME-LX) at 77 K. An oxygen-saturated MeCN solution of $AcrH_2$ (5.0×10^{-2} mol dm^{-3}) was irradiated with an Ushio Model U1-501 Xenon lamp for 1 h at 77 K. The photolysis of an oxygen-saturated MeCN solution of Acr=O (2.0×10^{-2} mol dm^{-3}) in the presence of H_2O (1.0 mol dm^{-3}) was also carried out for 30 min at 77 K. The e.s.r. spectra were recorded under non-saturating microwave power conditions. The g-value of e.s.r. spectrum was calibrated by using an Mn^{2+} e.s.r. marker.

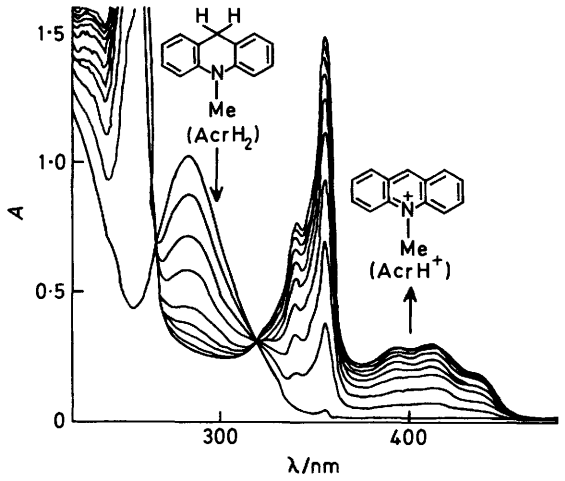

Figure 1. Electronic spectra observed in the photo-oxidation of $AcrH_2$ (5.6×10^{-5} mol dm^{-3}) by oxygen (2.6×10^{-3} mol dm^{-3}) in the presence of $HClO_4$ (1.0×10^{-3} mol dm^{-3}) and H_2O (2.6 mol dm^{-3}) in MeCN irradiated with light (220 nm $< \lambda <$ 440 nm); each spectrum was measured at intervals of 30 s.

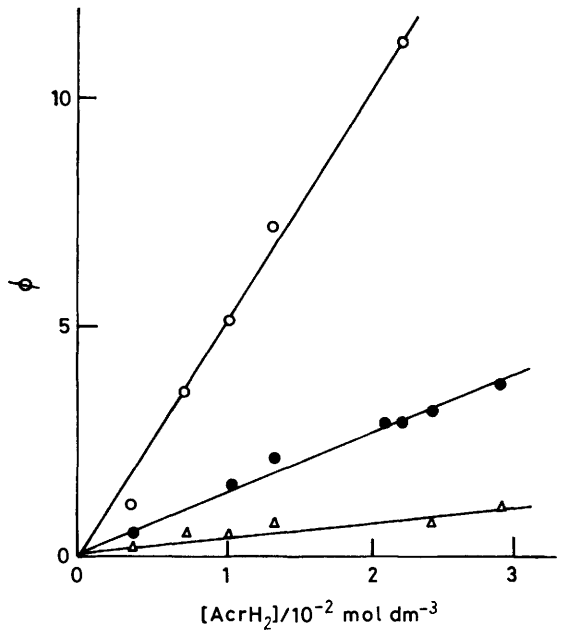

Figure 2. Dependence of the quantum yield on the $AcrH_2$ concentration for the photo-oxidation of $AcrH_2$ by oxygen (2.6×10^{-3} mol dm^{-3}) in the presence of $HClO_4$ (1.0×10^{-3} mol dm^{-3}) and H_2O (2.6 mol dm^{-3}) in MeCN (light: 220 nm $< \lambda <$ 440 nm); light intensity (*In*) 3.4×10^{-7} (○), 5.5×10^{-6} (●), and 3.4×10^{-5} (△) einstein s^{-1} dm^{-3}.

Results and Discussion

Photo-oxidation of $AcrH_2$ *by Oxygen in the Presence of Acid in MeCN.*—When an air-saturated MeCN solution containing $AcrH_2$, $HClO_4$, and H_2O is irradiated with u.v. light (220 nm $< \lambda <$ 440 nm), an absorption band due to $AcrH^+$ ($\lambda_{max.}$ = 358 nm) appears and the absorbance increases with the concomitant disappearance of the absorption band due to $AcrH_2$ ($\lambda_{max.}$ = 285 nm), as shown in Figure 1. The presence of H_2O is necessary in order to prevent the protonation of $AcrH_2$ by $HClO_4$ in MeCN, which would cause the disappearance of the absorption band due to $AcrH_2$.[9] The quantitative formation of $AcrH^+$ has also been confirmed by the measurement of ^1H n.m.r. spectra (see the Experimental section). After the completion of the photochemical reaction, an approximately equivalent amount of hydrogen peroxide (95% based on the initial amount of $AcrH_2$) was formed (see the Experimental section). Thus, the stoicheiometry of the photochemical reaction is given by equation (7).

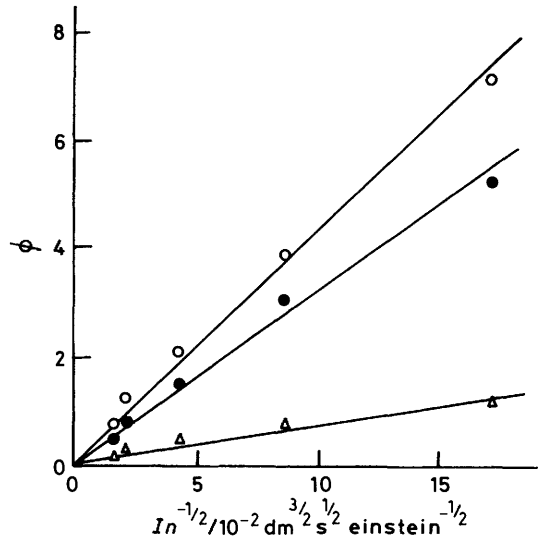

Figure 3. Dependence of the quantum yield on the light intensity (*In*) for the photo-oxidation of $AcrH_2$ by oxygen (2.6×10^{-3} mol dm^{-3}) in the presence of $HClO_4$ (1.0×10^{-3} mol dm^{-3}) and H_2O (2.6 mol dm^{-3}) in MeCN (light: 220 nm $< \lambda <$ 440 nm); $[AcrH_2] = 1.3 \times 10^{-2}$ (○), 1.0×10^{-2} (●), and 3.6×10^{-3} (△) mol dm^{-3}.

$$AcrH_2 + O_2 + H^+ \xrightarrow{h\nu} AcrH^+ + H_2O_2 \qquad (7)$$

The quantum yield for the photo-oxidation of $AcrH_2$ by oxygen in the presence of $HClO_4$ (1.0×10^{-3} mol dm^{-3}) in MeCN containing H_2O (2.6 mol dm^{-3}) is proportional to the concentration of $AcrH_2$ with each light intensity as shown in Figure 2, where the quantum yield exceeds unity for high concentrations of $AcrH_2$. In particular, when the light intensity absorbed by $AcrH_2$ is 3.4×10^{-7} einstein dm^{-3} s^{-1}, $\varphi = 11$. The dependence of φ on the light intensity at fixed $AcrH_2$ concentrations is shown in Figure 3, where the φ value is proportional to the reciprocal of the square root of light intensity for each concentration of $AcrH_2$. The large quantum yields exceeding unity in Figure 2, combined with the dependence of φ on the light intensity in Figure 3, strongly indicate that the photo-oxidation of $AcrH_2$ by oxygen in the presence of $HClO_4$ proceeds *via* radical-chain reactions, initiated by u.v. irradiation. The dependence of the quantum yield on the $HClO_4$ concentration is shown in Figure 4, where φ is constant with the variation in $[HClO_4]$; the photo-oxidation of $AcrH_2$ in the absence of $HClO_4$ in MeCN is described below.

The primary kinetic isotope effect φ_H/φ_D is determined by using $AcrD_2$ for the ratio of the rate of formation of $AcrH^+$ to that of $AcrD^+$. The φ_H/φ_D value is plotted against the logarithm of the concentration of $AcrH_2$ in Figure 5, where the φ_H/φ_D value is approximately unity in the region $[AcrH_2] < 10^{-4}$ mol dm^{-3} and increases gradually in the region $[AcrH_2] > 10^{-4}$ mol dm^{-3} to reach a constant value ($\varphi_H/\varphi_D = 3.0$) in the region $[AcrH_2] > 10^{-3}$ mol dm^{-3}. Such dependence of φ_H/φ_D on the $AcrH_2$ concentration suggests that the chain length remains close to unity for low $AcrH_2$ concentration ($< 10^{-3}$ mol dm^{-3}), while for high $AcrH_2$ concentration ($> 10^{-3}$ mol dm^{-3}) the chain length is sufficiently long for the φ_H/φ_D value to be determined

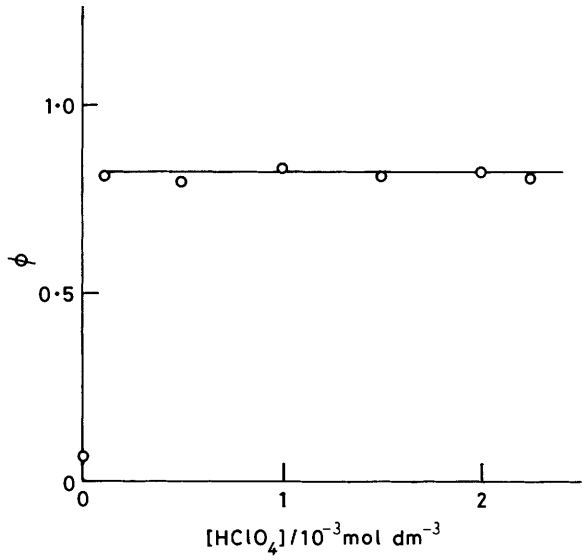

Figure 4. Dependence of the quantum yield on the $HClO_4$ concentration for the photo-oxidation of $AcrH_2$ by oxygen (2.6×10^{-3} mol dm^{-3}) in the presence of $HClO_4$ in MeCN containing H_2O (2.6 mol dm^{-3}) (light: 220 nm $< \lambda <$ 440 nm).

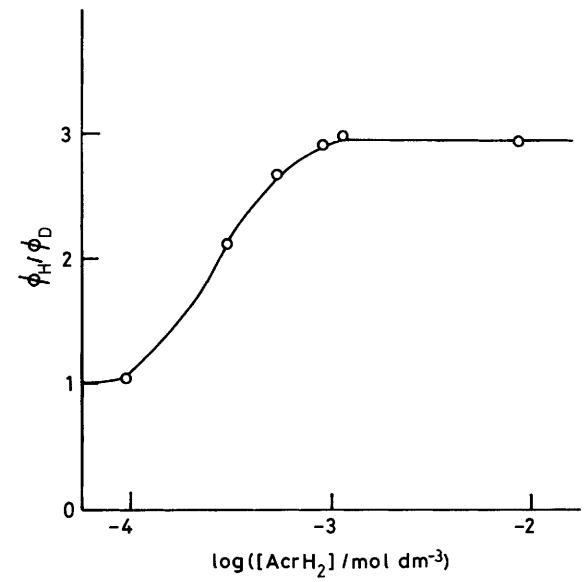

Figure 5. Dependence of the primary kinetic isotope effect (φ_H/φ_D) on the $AcrH_2$ concentration for the photo-oxidation of $AcrH_2$ by oxygen (2.6×10^{-3} mol dm^{-3}) in the presence of $HClO_4$ (1.0×10^{-3} mol dm^{-3}) and H_2O (2.6 mol dm^{-3}) in MeCN (light: 220 nm $< \lambda <$ 440 nm).

Table 1. Quenching rate constants (k_q) of the fluorescence of $AcrH_2$ by oxidants and the Gibbs energy change (ΔG^0_{et}) of the electron transfer from $^1AcrH_2^*$ to the oxidants in MeCN at 298 K.

Oxidant	ΔG^0_{et}/kJ mol^{-1}	k_q[a,b]/dm^3 mol^{-1} s^{-1}
Oxygen	-2.2×10^2	1.9×10^{10} (1.6×10^{10})
Fumaronitrile	-1.6×10^2	2.3×10^{10} (2.0×10^{10})
Diethyl fumarate	-1.5×10^2	1.6×10^{10} (1.8×10^{10})

[a] The experimental errors are within $\pm 10\%$. [b] The values in parentheses are those measured in the presence of $HClO_4$ (1.0×10^{-3} mol dm^{-3}).

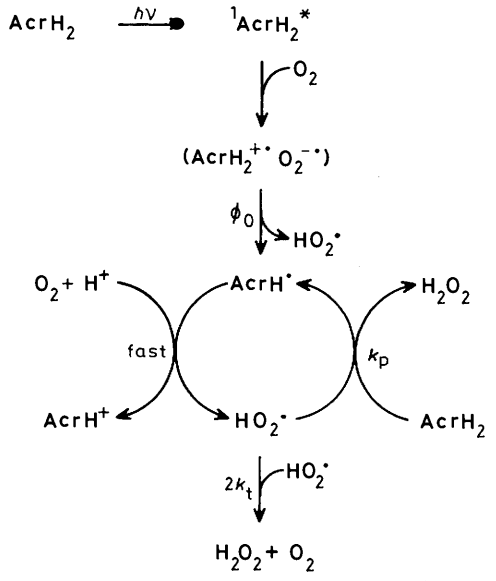

Scheme 1.

mainly by the propagation step in which the abstraction of hydrogen from $AcrH_2$ or $AcrD_2$ may be involved.

The excitation of an MeCN solution of $AcrH_2$ at 285 nm in both the presence and absence of $HClO_4$ results in fluorescence ($\lambda_{max.}$ = 385 nm). The quenching rate constants k_q have been determined from the Stern–Volmer plots [equation (6)]. The k_q values are listed in Table 1, together with the values of Gibbs-energy change of electron transfer from the singlet excited state of $AcrH_2$ to the oxidants (ΔG^0_{et}), which were determined from the oxidation potential of $^1AcrH_2^*$ ($E^0_{ox} = -3.1$ V), which is obtained by subtracting the zero–zero transition energy (3.9 eV) from the E^0_{ox} value of the ground state $AcrH_2$ [0.80 V)[10]] and the reduction potentials of oxidants (E^0_{red}).[10,19] The electron transfer from $^1AcrH_2^*$ to any oxidant in Table 1 is highly exothermic, and thus the k_q values of the oxidants in both the presence and absence of $HClO_4$ are diffusion limited.

Based on the above results, the radical-chain mechanism for the photo-oxidation of $AcrH_2$ by oxygen in the presence of $HClO_4$ may be given by Scheme 1. In the initiation step, the excitation of $AcrH_2$ results in the formation of the singlet state of $AcrH_2$ ($^1AcrH_2^*$), which transfers an electron to O_2 to produce the radical-ion pair ($AcrH_2^{+\bullet}$ $O_2^{-\bullet}$) which may dissociate to yield AcrH$^\bullet$ and $HO_2^\bullet$ by the facile proton transfer from $AcrH_2^{+\bullet}$ to $O_2^{-\bullet}$. In the propagation step, $HO_2^\bullet$ abstracts a hydrogen atom from $AcrH_2$ to give H_2O_2 and AcrH$^\bullet$. The electron transfer from AcrH$^\bullet$ to O_2 is endothermic in MeCN, since the oxidation potential of AcrH$^\bullet$ (-0.43 V)[10] is more positive than the reduction potential of O_2 (-0.86 V).[20] In the presence of $HClO_4$, however, the reduction potential of O_2 may be shifted in the positive direction,[21] thus it is possible that AcrH$^\bullet$ transfers an electron to O_2 to yield $AcrH^+$, regenerating $HO_2^\bullet$ (Scheme 1). The termination step is the disproportionation of $HO_2^\bullet$ to yield H_2O_2 and O_2 (Scheme 1).

By applying the steady-state approximation to the radical species ($HO_2^\bullet$ and AcrH$^\bullet$) in Scheme 1, the quantum yield (φ) is given as the function of the light intensity (In) and the concentration of $AcrH_2$ [equation (8)], where φ_0 is the quantum

$$\varphi = k_p(\varphi_0/k_t In)^{\frac{1}{2}}[AcrH_2] \quad (8)$$

yield of the initiation step, k_p is the rate constant of the rate-determining propagation step, and k_t is the rate constant of the termination step. Equation (8) agrees well with the experimental

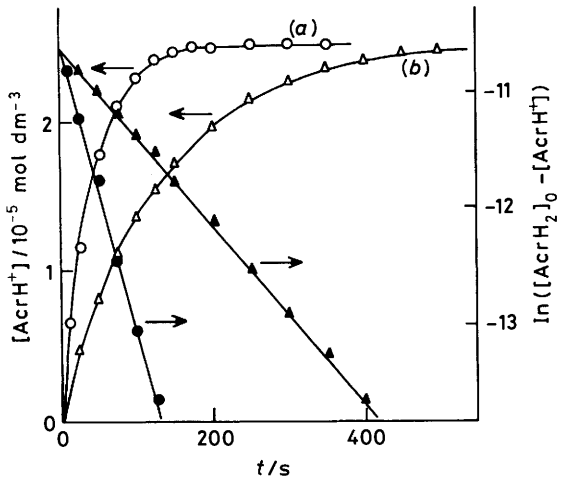

Figure 6. (*a*) Formation of $AcrH^+$ in the oxidation of $AcrH_2$ ○ and $AcrD_2$ △ by oxygen in the presence of $FeCl_2$ (1.1×10^{-4} mol dm^{-3}), H_2O_2 (4.9×10^{-2} mol dm^{-3}), and $HClO_4$ (1.0×10^{-3} mol dm^{-3}) in MeCN containing H_2O (2.6 mol dm^{-3}); (*b*) the pseudo-first-order plots.

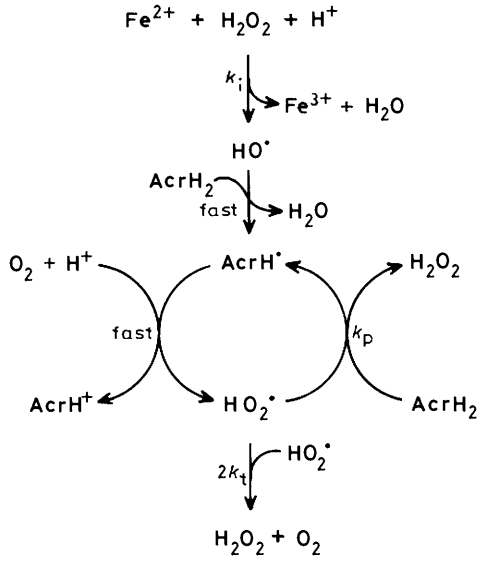

Scheme 2.

result that the φ value is proportional to the $AcrH_2$ concentration (Figure 2) and to the reciprocal of the square root of the light intensity (Figure 3), and is independent of the $HClO_4$ concentration (Figure 4). The absence of the primary kinetic isotope effect ($\varphi_H/\varphi_D = 1.0 \pm 0.1$) and its presence ($\varphi_H/\varphi_D = 3.0 \pm 0.3$) in the low and high concentrations of $AcrH_2$, respectively (Figure 5), are also consistent with Scheme 1, since no primary kinetic isotope effect is expected at low $AcrH_2$ concentrations when the chain length is close to unity and the rate is mainly determined by the electron transfer from $^1AcrH_2^*$ to oxygen, while an appreciable primary kinetic isotope effect is expected at high $AcrH_2$ concentrations when the chain length is sufficiently long for the rate to be mainly determined by the chain-propagation step in which the hydrogen abstraction of $HO_2^•$ from $AcrH_2$ or $AcrD_2$ is involved. The primary kinetic isotope effect of the hydrogen abstraction of $HO_2^•$ from $AcrH_2$ is also examined independently below.

Oxidation of $AcrH_2$ *by Oxygen, Initiated by the Fenton Reaction.*—Although $AcrH_2$ is thermally stable to oxygen, as

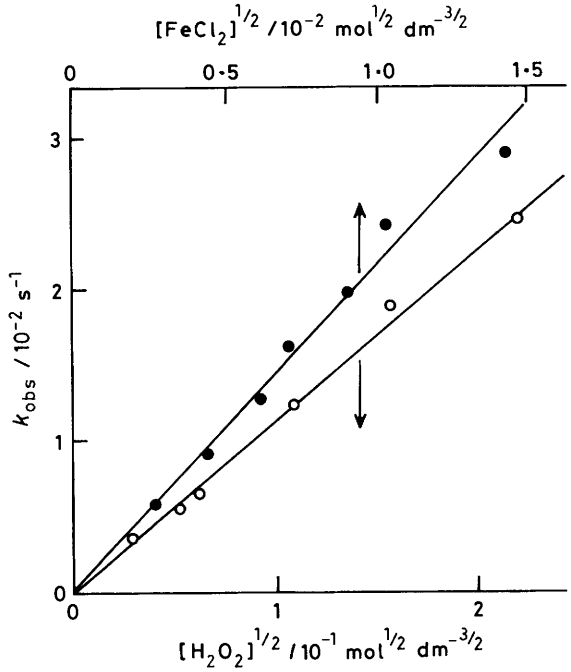

Figure 7. Plots of k_{obs} *vs.* $[FeCl_2]^{\frac{1}{2}}$ and $[H_2O_2]^{\frac{1}{2}}$ for the oxidation of $AcrH_2$ by oxygen in the presence of $FeCl_2$, H_2O_2, and $HClO_4$ (1.9×10^{-3} mol dm^{-3}) in MeCN containing H_2O (2.6 mol dm^{-3}) at 298 K.

well as H_2O_2, in the absence of $HClO_4$ in MeCN containing H_2O (2.6 mol dm^{-3}), the addition of $FeCl_2$ and $HClO_4$ results in the facile oxidation of $AcrH_2$ to $AcrH^+$. The rate of formation of $AcrH^+$ obeys pseudo-first-order kinetics under conditions such that the concentrations of oxygen, H_2O_2, and $HClO_4$ are maintained at >tenfold excess of the concentration of $AcrH_2$ as shown in Figure 6. When $AcrH_2$ is replaced by the 9,9′-dideuteriated analogue ($AcrD_2$), the pseudo-first-order rate constant k_{obs} obtained from the slope of the plot in Figure 6(*b*) is smaller than the corresponding value of $AcrH_2$, demonstrating the presence of a primary kinetic isotope effect, $k_H/k_D = 3.2 \pm 0.3$, which is essentially the same as that observed in the photo-oxidation of $AcrH_2$ by oxygen at the high $AcrH_2$ concentrations (Figure 5). This value is also compatible with the reported k_H/k_D value for the hydrogen abstraction of $HO_2^•$ from BNAH observed in the autoxidation of BNAH in the presence of *N*,*N*,*N*′,*N*′-tetramethyl-1,4-phenylenediamine in an aqueous solution.[22]

It is well known that the Fenton reagent (Fe^{2+} and H_2O_2) produces the hydroxyl radical (HO•), which may convert $AcrH_2$ into AcrH• as shown in Scheme 2, where the subsequent reactions are the same as those in Scheme 1. In the same manner as the case for Scheme 1, the rate of formation of $AcrH^+$ is given by equation (9), where k_i is the initiation rate constant of the

$$d[AcrH^+]/dt = k_p[AcrH_2](k_i/k_t)^{\frac{1}{2}}[FeCl_2]^{\frac{1}{2}}[H_2O_2]^{\frac{1}{2}} \quad (9)$$

Fenton reaction and the other rate constants (k_p and k_t) are the same as in equation (8). The dependence of k_{obs} on the $FeCl_2$ and H_2O_2 concentrations in equation (9) is confirmed as shown in Figure 7, where k_{obs} is proportional to $[FeCl_2]^{\frac{1}{2}}$ and $[H_2O_2]^{\frac{1}{2}}$. Thus, the agreement of the primary kinetic isotope effects between the photochemical (Figure 5) and thermal (Figure 6) radical chain reactions confirms that the chain carrier in both cases is the $HO_2^•$ radical.

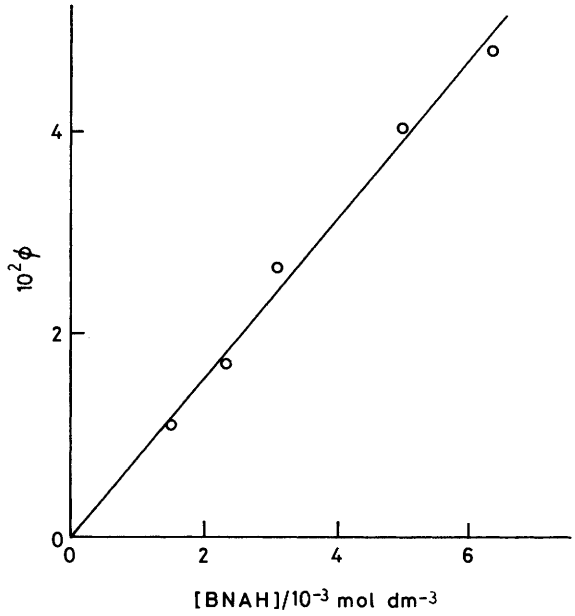

Figure 8. Dependence of the quantum yield (φ) on the BNAH concentration for the photo-oxidation of BNAH by oxygen ([O_2] = 2.5 × 10^{-4} mol dm^{-3}) in an aqueous buffer solution (pH 7) (light: 220 nm < λ < 440 nm); light intensity: 3.4 × 10^{-5} einstein s^{-1} dm^{-3}.

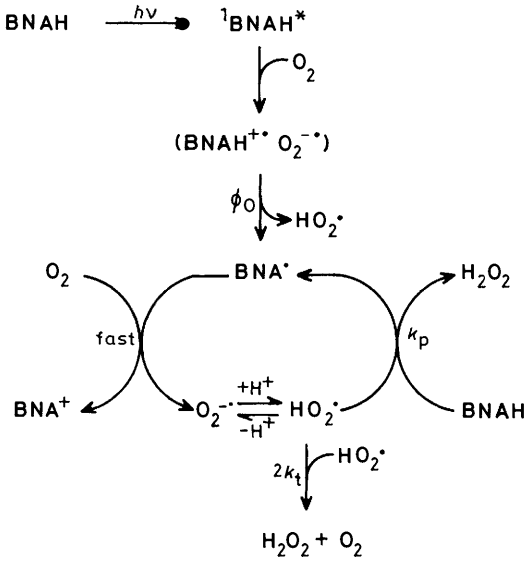

Scheme 3.

Photo-oxidation of BNAH by Oxygen in an Aqueous Solution.—When an air-saturated aqueous buffer solution containing BNAH is irradiated with u.v. light (220 nm < λ < 440 nm), an absorption band due to BNA^+ ($\lambda_{max.}$ = 270 nm) appears and the absorbance increases with the concomitant disappearance of the absorption band due to BNAH ($\lambda_{max.}$ = 350 nm). The quantum yield for the photo-oxidation of BNAH by oxygen is proportional to the concentration of BNAH (Figure 8), as is the case for the photo-oxidation of $AcrH_2$ by oxygen in the presence of $HClO_4$ (Figure 2).

The radical chain mechanism for the photo-oxidation of BNAH by oxygen may be given by Scheme 3, which is essentially the same as Scheme 1, except for the propagation step where BNA$^\bullet$ can transfer an electron to O_2 to yield BNA^+ and $O_2^{-\bullet}$ in the absence of acid, since the electron transfer from

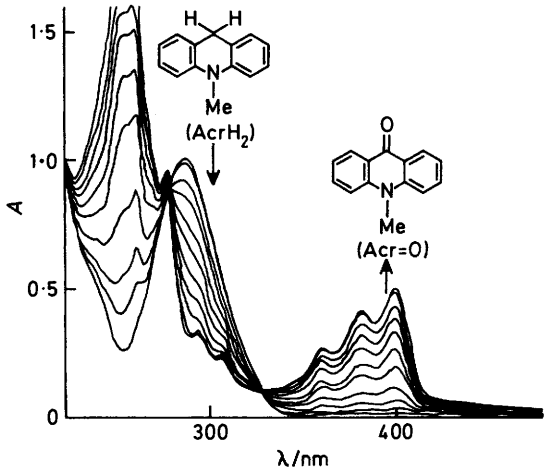

Figure 9. Electronic spectra observed in the photo-oxidation of $AcrH_2$ (5.6×10^{-5} mol dm^{-3}) by oxygen in air-saturated MeCN (light: 220 nm < λ < 440 nm), [O_2] = 2.6×10^{-3} mol dm^{-3}; each spectrum is measured at 1 min intervals.

BNA$^\bullet$ to oxygen is highly exothermic based on the one electron oxidation potential of BNA$^\bullet$ (−1.08 V)[10] and the one-electron reduction potential of O_2 (−0.4 V)[21] in a neutral aqueous solution. The hydroperoxyl radical $HO_2^\bullet$, which exists in equilibrium with $O_2^{-\bullet}$, can abstract hydrogen from BNAH to yield H_2O_2, regenerating BNA$^\bullet$. According to Scheme 3, the quantum yield is proportional to the BNAH concentration, in agreement with the experimental observation in Figure 8. The smaller φ value in the case of BNAH (Figure 8) than the case of $AcrH_2$ (Figure 2) may be ascribed to the unfavourable equilibrium for $HO_2^\bullet$ (pK_a = 4.7)[21] in a neutral aqueous solution where $O_2^{-\bullet}$ predominates (>99%), and also to the less efficient quenching of ^{1}BNAH* than $^1AcrH_2^*$ due to the shorter lifetime of the former (τ 0.76 ns);[18,23] for the latter τ 14 ns.[18]

Photo-oxidation of $AcrH_2$ *by Oxygen in the Absence of Acid in* MeCN.—When an air-saturated MeCN solution containing $AcrH_2$ in the absence of $HClO_4$ is irradiated with u.v. light (220 nm < λ < 440 nm), the absorption band due to Acr=O ($\lambda_{max.}$ 440 nm) appears and the absorbance increases with the concomitant disappearance of the absorption band due to $AcrH_2$ ($\lambda_{max.}$ 285 nm), as shown in Figure 9. The quantitative formation of Acr=O has also been confirmed by the measurement of ^{1}H n.m.r. spectra (see the Experimental section). After the completion of the photochemical reaction, a somewhat smaller amount of hydrogen peroxide than that for Acr=O (60% based on the initial amount of $AcrH_2$) was detected (see the Experimental section), probably because of the photo-decomposition of hydrogen peroxide under prolonged irradiation by u.v. light. Thus, the stoicheiometry of the photochemical reaction may be given by equation (10).

$$AcrH_2 + \tfrac{3}{2}O_2 \xrightarrow{h\nu} Acr{=}O + H_2O_2 \qquad (10)$$

Conversely, for the case of the photo-oxidation of $AcrH_2$ by oxygen in the presence of $HClO_4$ (Figures 2 and 3), the quantum yield for the photo-oxidation of $AcrH_2$ by oxygen in the absence of $HClO_4$ is independent of the concentration of $AcrH_2$ and the light intensity, as shown in Figure 10.

In order to detect the reactive intermediate produced in this photochemical reaction, the e.s.r. spectra were measured after the u.v. irradiation of an oxygen-saturated MeCN solution of $AcrH_2$ at 77 K (see the Experimental section). The result is shown in Figure 11(*a*), where the isotropic signal at g = 2.0036 ± 0.0002 is observed, together with the small aniso-

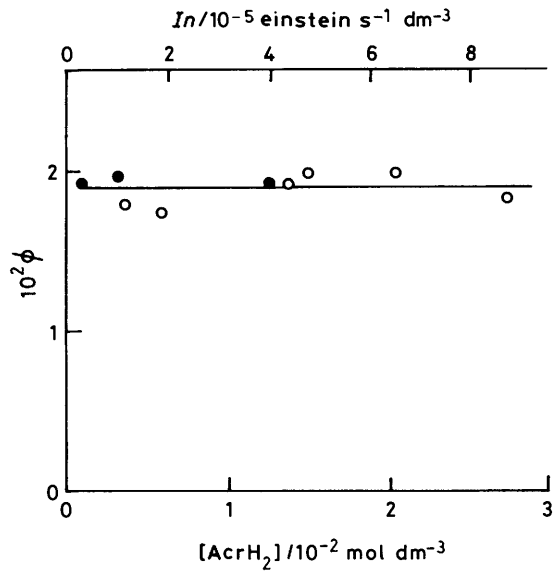

Figure 10. Depedence of the quantum yield on the $AcrH_2$ concentration (○) and the light intensity (●) for the photo-oxidation of $AcrH_2$ by oxygen (2.6×10^{-3} mol dm^{-3}) in MeCN (light: 220 nm < λ < 440 nm).

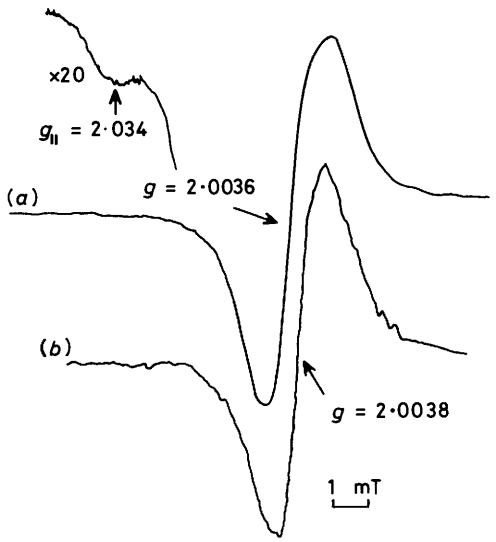

Figure 11. E.s.r. spectrum observed (*a*) after the irradiation of an oxygen-saturated MeCN solution containing $AcrH_2$ (5.0×10^{-2} mol dm^{-3}) with u.v. light for 1 h at 77 K; (*b*) after the irradiation of an MeCN solution containing Acr=O (2.0×10^{-2} mol dm^{-3}) and H_2O (1.0 mol dm^{-3}) for 30 min at 77 K.

tropic signal ($g_{\parallel}$ 2.034 ± 0.001), due to $AcrHO_2^{\bullet}$, characteristic of alkylperoxy radicals.[24] No appreciable amount of $HO_2^{\bullet}$, which can be readily identified by the large proton hyperfine structure ($A_{\parallel}$ 1.35 and $A_{\perp}$ 0.86 mT),[25] was observed. Essentially the same isotropic signal as in Figure 11(*a*) was observed at g = 2.0038 ± 0.0002 in the photolysis of Acr=O in the presence of H_2O, as shown in Figure 11(*b*) (see the Experimental section). The excitation of a carbonyl compound is known to result in the abstraction of hydrogen from a solvent to yield the corresponding alcohol radical (ĊOH).[26] Thus, the isotropic e.s.r. signal in Figure 11(*a*) may be tentatively assigned to $AcrOH^{\bullet}$.[26,27]

On the basis of the above results, the mechanism of the photo-oxidation of $AcrH_2$ by oxygen in the absence of $HClO_4$ may be given by Scheme 4. The excitation of $AcrH_2$ results in the formation of singlet-state $AcrH_2$ ($^1AcrH_2^*$), which transfers an

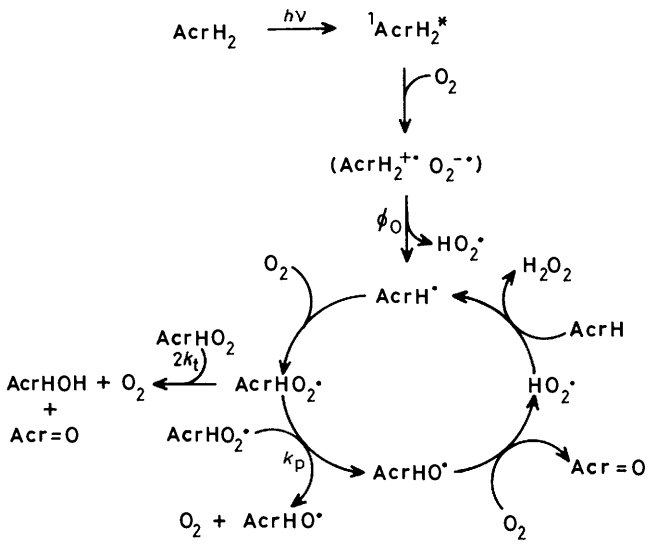

Scheme 4.

electron to O_2 to produce the radical-ion pair ($AcrH_2^{+\bullet}$ $O_2^{-\bullet}$). The radical ion pair may dissociate to yield $AcrH^{\bullet}$ and $HO_2^{\bullet}$ by proton transfer from $AcrH_2^{+\bullet}$ to $O_2^{-\bullet}$. In the absence of $HClO_4$, an electron transfer from $AcrH^{\bullet}$ to O_2 is endothermic, shown by the oxidation potential of $AcrH^{\bullet}$ and the reduction potential of O_2 in MeCN (−0.43 V[10] and −0.86 V,[20] respectively). Thus, in the propagation step, the addition of oxygen to $AcrH^{\bullet}$, instead of electron transfer, may occur to yield acridinyl peroxyl radical $AcrHO_2^{\bullet}$ as detected by e.s.r. spectroscopy [Figure 11(*a*)]. The bimolecular reaction of $AcrHO_2^{\bullet}$ gives $AcrOH^{\bullet}$ and O_2, the former of which is also detected by e.s.r. measurement [Figure 11(*a*)]. The $AcrOH^{\bullet}$, which is a carbon-centre radical, may react with O_2 to yield Acr=O and $HO_2^{\bullet}$, the latter of which can abstract hydrogen from $AcrH_2$ to yield H_2O_2, accompanied by regeneration of $AcrH^{\bullet}$. The termination step may be the disproportionation of $AcrHO_2^{\bullet}$ to give Acr=O, AcrHOH, and O_2. According to Scheme 4, the stoicheiometry of the photo-oxidation agrees with the experimental results [equation (10)]. By applying the steady-state approximation to the reactive intermediates ($AcrH^{\bullet}$, $AcrHO_2^{\bullet}$, $AcrOH^{\bullet}$, and $HO_2^{\bullet}$) in Scheme 4, the quantum yield may be given by equation (11), where the φ

$$\varphi = 2\varphi_0 k_p/k_t \qquad (11)$$

value is independent of the concentration of $AcrH_2$ and the light intensity, which agrees with the experimental results in Figure 10.

RFTA-sensitized Photo-oxidation of $AcrH_2$ *by Oxygen.*— When an argon-saturated MeCN–H_2O (5:1 v/v) solution containing RFTA (8.0×10^{-4} mol dm^{-3}), $AcrH_2$ (8.9×10^{-3} mol dm^{-3}), and $HClO_4$ (1.0×10^{-2} mol dm^{-3}) is irradiated with visible light (λ > 400 nm), the absorption band due to F1 ($\lambda_{max.}$ = 444 nm) disappears with the concomitant appearance of the absorption band due to $AcrH^+$. Upon introducing oxygen into the resulting solution, the facile regeneration of RFTA was observed. Thus, the excited state of RFTA can oxidize $AcrH_2$ to $AcrH^+$ under visible light irradiation when RFTA may be reduced to $RFTAH_2$, which is readily oxidized by oxygen to regenerate RFTA.[16] In fact, $AcrH_2$ (3.2×10^{-3} mol dm^{-3}) is readily oxidized by oxygen in the presence of a catalytic amount of RFTA (9.2×10^{-5} mol dm^{-3}) under visible light irradiation, although no photo-oxidation of $AcrH_2$ by oxygen occurs in the absence of RFTA under otherwise identical conditions.

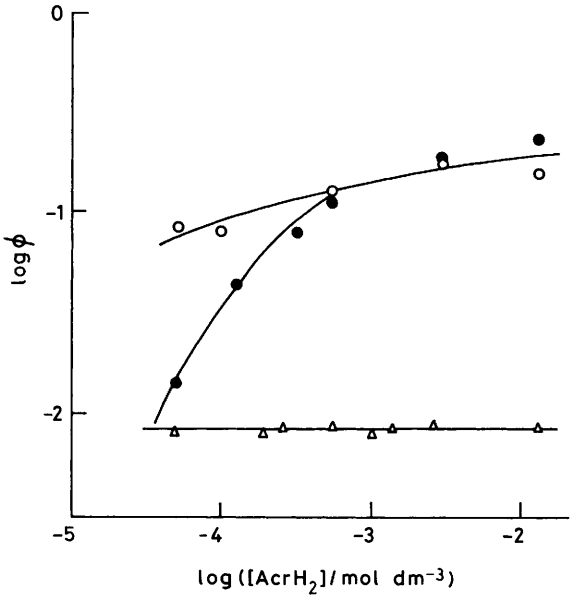

Figure 12. Plots of log φ *vs.* log[$AcrH_2$] for the photochemical reaction of $AcrH_2$ with RFTA (9.2×10^{-5} mol dm^{-3}) in the absence of oxygen (△), in the presence of air (○) and oxygen (●) in MeCN–H_2O (5:1 v/v) (light: λ > 400 nm).

Table 2. Primary kinetic isotope effects (φ_H/φ_D) for the photochemical reactions of $AcrH_2$ and $AcrD_2$ with RFTA (9.2×10^{-5} mol dm^{-3}) in the absence and presence of oxygen in MeCN–H_2O (5:1 v/v) containing $HClO_4$ (1.0×10^{-3} mol dm^{-3}) under visible light irradiation (λ > 400 nm).

[$AcrH_2$] or [$AcrD_2$]/ mol dm^{-3}	φ_H/φ_D [a,b]	φ_H/φ_D [a,c]
3.6×10^{-5}	4.8	1.8
3.6×10^{-4}	4.5	1.8 (1.5)[d]
3.6×10^{-3}	4.4	1.8 (1.5)[d]
1.5×10^{-2}	4.3	1.6 (1.6)[d]

[a] The experimental error is ±10%. [b] Under argon at atmospheric pressure. [c] Under oxygen at atmospheric pressure unless otherwise noted. [d] Under air at atmospheric pressure.

The logarithm of the quantum yield for the photochemical reactions of RFTA with $AcrH_2$ in the presence of $HClO_4$ (1.0×10^{-3} mol dm^{-3}) under argon, air, and oxygen at atmospheric pressure are plotted, as a function of log[$AcrH_2$] in Figure 12. The quantum yield in the absence of oxygen is constant even in the low concentration range of $AcrH_2$ ($< 10^{-4}$ mol dm^{-3}). Thus, the minimum lifetime (τ) of the excited state of RFTA is estimated to be τ > 1 μs by assuming that the reaction between the excited state of RFTA and $AcrH_2$ is diffusion limited. Such a long lifetime indicates that the excited state of RFTA involved in the photo-oxidation of $AcrH_2$ by RFTA is the triplet state (^{3}RFTA*), since the lifetimes of the singlet[28] and triplet[29] excited states of flavin analogues are known to be 10^{-9} and *ca.* 10^{-4}–10^{-5} s, respectively. In the presence of oxygen, the φ value increases with increasing $AcrH_2$ concentration to reach a constant value in the high $AcrH_2$ concentration ($> 5 \times 10^{-4}$ mol dm^{-3}). The constant φ value in the presence of oxygen is significantly larger than the φ value in the absence of oxygen.

The primary kinetic isotope effects φ_H/φ_D in these reactions were determined by using $AcrD_2$ as the ratio of the rate of formation of $AcrH^+$ to that of $AcrD^+$. The φ_H/φ_D values are listed at various concentrations of $AcrH_2$ in the presence and absence of oxygen in Table 2. The φ_H/φ_D values in the absence of oxygen are always larger than those in the presence of oxygen.

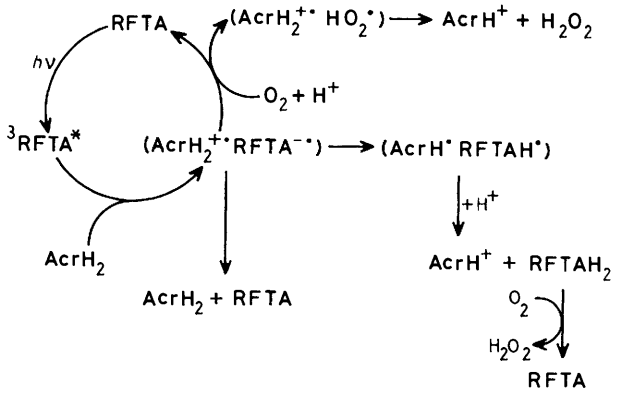

Scheme 5.

Kaptein *et al.*[3] has reported that NADH can transfer an electron to the triplet excited state of a flavin analogue to produce the radical-ion pair on the basis of the CIDNP study, which suggests also that NAD^+ is formed mainly *via* the radical-ion pair in the absence of oxygen. The present kinetic results in Figure 12 as well as the kinetic isotope effect (Table 2) support the conclusion of the CIDNP study[3] as follows.

The reaction mechanism of the photo-oxidation of $AcrH_2$ by RFTA in the absence and presence of oxygen is shown in Scheme 5. Firstly, electron transfer from $AcrH_2$ to ^{3}RFTA* may occur to produce the radical ion pair ($AcrH_2^{+\cdot}$ $RFTA^{-\cdot}$), followed by the proton transfer from $AcrH_2^{+\cdot}$ to $RFTA^{-\cdot}$ in the cage to give AcrH· and RFTAH·. Secondly, electron transfer from AcrH· to RFTAH· takes place to give the products $AcrH^+$ and $RFTAH_2$ in the presence of $HClO_4$ in MeCN/H_2O. The electron transfer is exothermic as shown by the fact that the one-electron oxidation potential of AcrH· (−0.43 V)[10] and the one-electron reduction potential of RFTAH· (the reduction potential of the flavosemiquinone radical in the presence of $HClO_4$ should be more positive than −0.41 V which is the value in the absence of $HClO_4$).[30] Thus, the kinetic isotope effect (φ_H/φ_D 4.5 ± 0.4 in Table 2) may correspond to that for the proton transfer from $AcrH_2^{+\cdot}$ to $RFTA^{-\cdot}$, which is also exothermic based on the difference of pK_a between $AcrH_2^{+\cdot}$ (2.0)[10] and the flavosemiquinone radical (7.0).[31] In such a case, the limiting quantum yield may be determined by the competition between the proton transfer from $AcrH_2^{+\cdot}$ to $RFTA^{-\cdot}$ and the back electron transfer from $RFTA^{-\cdot}$ to $AcrH_2^{+\cdot}$.

In the presence of oxygen, the back electron transfer from $RFTA^{-\cdot}$ to $AcrH_2^{+\cdot}$ may be prevented by the trapping of the radical $RFTA^{-\cdot}$ by oxygen in the presence of $HClO_4$ to product $HO_2^{\cdot}$, accompanied by regeneration of RFTA. Thus, the quantum yields in the presence of oxygen become larger than those in the absence of oxygen. The trapping of radical species by oxygen prior to the proton transfer may reduce the kinetic isotope effect in the presence of oxygen (φ_H/φ_D 1.7 ± 0.2), compared with that in the absence of oxygen (φ_H/φ_D 4.5 ± 0.4), as shown in Table 2. Alternatively, there is a possibility that the kinetic isotope effect is ascribed to the hydrogen abstraction of ^{3}RFTA* from $AcrH_2$ to produce directly the radical pair (AcrH· RFTAH·). In such a case, however, it is difficult to account for the decrease in the primary kinetic isotope effect in the presence of oxygen.

The constant quantum yield in the high concentration range of $AcrH_2$ ($> 5 \times 10^{-4}$ mol dm^{-3}) in the presence of oxygen (Figure 12) suggests that the involvement of the radical-chain reactions (Scheme 1) may be negligible in the case of flavin-catalysed photo-oxidation of $AcrH_2$ by oxygen because of the facile reaction between $AcrH_2^{+\cdot}$ and $HO_2^{\cdot}$ in the cage to yield

H_2O_2 and $AcrH^+$ (Scheme 5). The decrease in the quantum yield in the low concentration range of $AcrH_2$ ($< 5 \times 10^{-4}$ mol dm^{-3}) in Figure 12 suggests that the lifetime of $^3RFTA^*$ is decreased in the presence of oxygen by the energy transfer from $^3RFTA^*$ to O_2.[32]

References

1 R. C. Bohinski, 'Modern Concepts in Biochemistry,' 3rd edn., Allyn & Bacon, Boston, 1979, p. 457; L. Stryer, 'Biochemistry,' Freeman, New York, 1988, ch. 17.
2 V. Massey, G. Palmer, and D. P. Ballou, 'Oxidases and Related Redox Systems,' eds. T. E. King, H. S. Mason, and M. Morrison, University Park Press, Baltimore, MD, 1973, p. 25; C. Radziejewski, D. P. Ballou, and E. T. Kaiser, *J. Am. Chem. Soc.*, 1985, **107**, 3352.
3 P. J. Hore, A. Volbeda, K. Dijkstra, and R. Kaptein, *J. Am. Chem. Soc.*, 1982, **104**, 6262.
4 R. S. Bodaness and P. C. Chan, *J. Biol. Chem.*, 1977, **252**, 8554.
5 R. J. Land and A. J. Swallow, *Biochim. Biophys. Acta*, 1971, **234**, 34.
6 B. Czochralska, W. Kawczynski, G. Bartosz, and D. Shugar, *Biochim. Biophys. Acta*, 1984, **801**, 403.
7 M. L. Cunningham, J. S. Johnson, S. M. Giovanazzi, and M. J. Park, *Photochem. Photobiol.*, 1985, **42**, 125.
8 C. C. Johnston, J. L. Gardner, C. H. Suelter, and D. E. Metzler, *Biochemistry*, 1963, **2**, 689; C. S. Y. Kim and S. Chaykin, *ibid.*, 1968, **7**, 2339; P. van Eikeren, D. L. Grier, and J. Eliason, *J. Am. Chem. Soc.*, 1979, **101**, 7406.
9 S. Fukuzumi, M. Ishikawa, and T. Tanaka, *J. Chem. Soc., Chem. Commun.*, 1985, 1069; S. Fukuzumi, M. Ishikawa, and T. Tanaka, *Tetrahedron*, 1986, **42**, 1021.
10 S. Fukuzumi, S. Koumitsu, K. Hironaka, and T. Tanaka, *J. Am. Chem. Soc.*, 1987, **109**, 305.
11 D. Ostović, R. M. G. Roberts, and M. M. Kreevoy, *J. Am. Chem. Soc.*, 1983, **105**, 7629; P. Karrer, L. Szabo, H. J. V. Krishna, and R. Schwyzer, *Helv. Chim. Acta*, 1950, **33**, 294.
12 Y. Kyogoku and B. S. Yu, *Bull. Chem. Soc. Jpn.*, 1969, **42**, 1387.
13 C. G. Hatchard and C. A. Parker, *Proc. R. Soc. London, Ser. A.*, 1956, **235**, 518; J. G. Calvert and J. N. Pitts, 'Photochemistry,' Wiley, New York, 1966, p. 783.
14 D. D. Perrin, W. L. F. Armarego, and D. R. Perrin, 'Purification of Laboratory Chemicals,' Pergamon Press, New York, 1966.
15 R. D. Mair and A. J. Graupner, *Anal. Chem.*, 1964, **36**, 194.
16 S. Fukuzumi, S. Kuroda, and T. Tanaka, *J. Am. Chem. Soc.*, 1985, **107**, 3020.
17 S. Fukuzumi, K. Hironaka, and T. Tanaka, *J. Am. Chem. Soc.*, 1983, **105**, 4722.
18 S. Fukuzumi and T. Tanaka, 'Photoinduced Electron Transfer,' eds. M. A. Fox and M. Chanon, Elsevier, Amsterdam, 1988, ch. 10.
19 S. Fukuzumi, K. Hironaka, N. Nishizawa, and T. Tanaka, *Bull. Chem. Soc. Jpn.*, 1983, **56**, 2220.
20 D. T. Sawyer, T. S. Calderwood, K. Yamaguchi, and C. T. Angelis, *Inorg. Chem.*, 1983, **22**, 2577.
21 D. T. Sawyer and J. S. Valentine, *Acc. Chem. Res.*, 1981, **14**, 393.
22 E. J. H. Bechara and G. Gilento, *Biochemistry*, 1971, **10**, 1831.
23 F. M. Martens, J. W. Verhoeven, R. A. Gase, U. K. Pandit, and Th. J. de Bore, *Tetrahedron*, 1978, **34**, 443.
24 J. A. Howard, *Can. J. Chem.*, 1972, **50**, 1981; E. Melamud and B. L. Silver, *J. Magn. Reson.*, 1974, **14**, 112; E. Melamud, S. Schlick, and B. L. Silver, *ibid.*, 1974, **14**, 104.
25 M. Carlier and L.-R. Sochet, *J. Chem. Soc., Faraday Trans 1*, 1983, **79**, 815; S. J. Wyard, R. C. Smith, and F. J. Adrian, *J. Chem. Phys.*, 1968, **49**, 2780; F. J. Adrian, E. L. Cochran, and V. A. Bowers, *ibid.*, 1967, **47**, 5441; E. Saito and B. H. Bielski, *J. Am. Chem. Soc.*, 1961, **83**, 4467.
26 P. B. Ayscough, R. C. Sealy, and D. E. Woods, *J. Phys. Chem.*, 1971, **75**, 3454.
27 P. J. Krusic, P. Meakin, and J. P. Jesson, *J. Phys. Chem.*, 1971, **75**, 3438; A. J. Dobbs and R. O. C. Norman, *J. Chem. Soc., Perkin Trans. 2*, 1972, 786.
28 A. J. W. G. Visser and F. Müller, *Helv. Chim. Acta*, 1979, **62**, 593.
29 M. S. Grodowski, B. Veyret, and K. Weiss, *Photochem. Photobiol.*, 1977, **26**, 341; D. E. Edmonson, F. Rizzuto, and G. Tollin, *ibid.*, 1977, **25**, 445.
30 M. J. Clarke and M. G. Dowling, *Inorg. Chem.*, 1981, **20**, 3506.
31 K. H. Dudley, A. Ehrenberg, P. Hemmerich, and F. Müller, *Helv. Chim. Acta*, 1964, **47**, 1354.
32 P. F. Heelis, *Chem. Soc. Rev.*, 1982, **11**, 15.

Received 1*st August* 1988; *Paper* 8/03125H